Title

68Ga-PSMA-11 PET Imaging of Response to Androgen Receptor Inhibition: First Human Experience

Journal

Journal of Nuclear Medicine, 58(1)

ISSN

0161-5505

Authors

Hope, Thomas A
Truillet, Charles
Ehman, Eric C
et al.

Publication Date

2017

DOI

10.2967/jnumed.116.181800

Peer reviewed

^{68}Ga-PSMA-11 PET Imaging of Response to Androgen Receptor Inhibition: First Human Experience

Thomas A. Hope*[1–3], Charles Truillet*[1], Eric C. Ehman[4], Ali Afshar-Oromieh[5], Rahul Aggarwal[3,6], Charles J. Ryan[3,6], Peter R. Carroll[3,7], Eric J. Small[3,6], and Michael J. Evans[1]

[1]Department of Radiology and Biomedical Imaging, University of California, San Francisco, San Francisco, California; [2]Department of Radiology, San Francisco VA Medical Center, San Francisco, California; [3]Helen Diller Family Comprehensive Cancer Center, University of California, San Francisco, San Francisco, California; [4]Department of Radiology, Mayo Clinic, Rochester, Minnesota; [5]Department of Nuclear Medicine, Heidelberg University Hospital, Heidelberg, Germany; [6]Division of Hematology/Oncology, Department of Medicine, University of California, San Francisco, San Francisco, California; and [7]Department of Urology, University of California, San Francisco, San Francisco, California

The purpose of this work was to evaluate the effect of androgen receptor (AR) inhibition on prostate-specific membrane antigen (PSMA) uptake imaged using ^{68}Ga-PSMA-11 PET in a mouse xenograft model and in a patient with castration-sensitive prostate cancer. **Methods:** We imaged 3 groups of 4 mice bearing LNCaP-AR xenografts before and 7 d after treatment with ARN-509, orchiectomy, or control vehicle. Additionally, we imaged one patient with castration-sensitive prostate cancer before and 4 wk after treatment with androgen deprivation therapy (ADT). Uptake on pre- and post-treatment imaging was measured and compared. **Results:** PSMA uptake increased 1.5- to 2.0-fold in the xenograft mouse model after treatment with both orchiectomy and ARN-509 but not with vehicle. Patient imaging demonstrated a 7-fold increase in PSMA uptake after the initiation of ADT. Thirteen of 22 lesions in the imaged patient were visualized on PSMA PET only after treatment with ADT. **Conclusion:** Inhibition of the AR can increase PSMA expression in prostate cancer metastases and increase the number of lesions visualized using PSMA PET. The effect seen in cell and animal models can be recapitulated in humans. A better understanding of the temporal changes in PSMA expression is needed to leverage this effect for both improved diagnosis and improved therapy.

Key Words: oncology: GU; PET; androgen receptor; PSMA PET; prostate cancer

J Nucl Med 2017; 58:81–84
DOI: 10.2967/jnumed.116.181800

Prostate-specific membrane antigen (PSMA) is a 100-kD transmembrane glycoprotein that is overexpressed on nearly all prostate cancers, particularly poorly differentiated and metastatic lesions (*1–3*). During the past 2 y, there have been literature reports of more than 1,000 patients imaged using PSMA ligands in studies that focused on the ability to detect metastases in patients with biochemical recurrence and demonstrated an improved detection rate compared with choline PET or other conventional imaging modalities (*4–9*).

Unlike ^{18}F-FDG, PSMA expression does not correlate positively with disease progression. In fact, cellular PSMA expression is regulated by the androgen receptor (AR), which is frequently targeted during prostate cancer treatments and can therefore confound interpretation. As opposed to prostate-specific antigen levels, PSMA expression on the cell surface increases with AR inhibition (*10–12*). Previous work by Evans et al. in mice bearing PSMA-expressing xenografts demonstrated that PSMA expression is increased with both orchiectomy and enzalutamide (*11*), a finding that has recently been reproduced in multiple prostate cancer cell lines and circulating tumor cells (*13,14*).

We hypothesized that inhibition of the AR will result in a transient increase in PSMA expression on prostate cancer cells. First, using ^{68}Ga-PSMA-11 PET, we evaluated the effect of AR-targeted therapies in a xenograft model. Second, since over 90% of patients initially respond to androgen deprivation therapy (ADT), we chose a patient with castration-sensitive metastatic disease for an in vivo test of our hypothesis that AR inhibition will increase PSMA expression (*15*).

MATERIALS AND METHODS

^{68}Ga-PSMA-11 Labeling Procedure

^{68}Ga was obtained by eluting a ^{68}Ge/^{68}Ga generator (iTG) yielding radioactivity in the range of 555–1,110 MBq (15–30 mCi) during synthesis. The syntheses were conducting using an iQS ^{68}Ga fluidic labeling module (RadioMedix Inc.). Precursor (DKFZ-PSMA-11) or Glu-NH-CO-NH-Lyx(Ahx)-HBED-CC, where HBED-CC is *N,N′*-bis[2-hydroxy-5-(carboxyethyl)-benzyl]ethylenediamine-*N,N′*-diacetic acid, was purchased from ABX Advanced Biochemical Compounds. All reagents for formulating the final product were provided in a kit from ABX.

The precursor was dispensed into 5-μg aliquots dissolved in 100 μL of 0.25 M sodium acetate buffer and stored at −20°C until use. The precursor (made up to a total of 1 mL with sodium acetate buffer) was added to the preheated reaction vessel (100°C–110°C), and the generator was immediately eluted into the reaction vessel. The contents were heated for 5 min, after which they were pushed through an activated C18 Sep-Pak Light cartridge (Waters) and directed to a waste vial. The reaction vessel was further washed with 5 mL of saline, which was directed to a waste vial. The product was then eluted with 1 mL of 60% ethanol in water followed by 10 mL of saline and passed through a

Received Jul. 28, 2016; revision accepted Aug. 28, 2016.
For correspondence or reprints contact: Michael J. Evans, 185 Berry St., Lobby 6, Ste. 350, Department of Radiology and Biomedical Imaging, University of California, San Francisco, San Francisco, CA 94107.
E-mail: michael.evans@ucsf.edu
*Contributed equally to this work.
Published online Sep. 22, 2016.

sterilizing filter. Typical yields are based on the total ^{68}Ga eluted and range from 85% to 90%.

Animal Experiment

Our prior data showing that upregulation of PSMA can be quantified with PET were acquired with ^{64}Cu-labeled J591. Because J591 is a full-sized monoclonal antibody with a long residence time in blood, it was not obvious whether changes in PSMA could be measured with a more rapidly clearing agent such as ^{68}Ga-PSMA-11. Therefore, we measured relative changes in PSMA expression with ^{68}Ga-PSMA-11 in mice bearing LNCaP-AR xenografts. Twelve 3- to 5-wk-old male *nu/nu* mice obtained from Charles River were studied: 4 treated with vehicle, 4 with orchiectomy, and 4 with apalutamide (ARN-509), which is a nonsteroidal competitive AR inhibitor. LnCAP-AR cells (5×10^7) in a 1:1 mixture (v/v) of medium and Matrigel (Corning) were subcutaneously inoculated into one flank. Tumors were palpable within 20–30 d after injection. Surgical castration was performed according to our Institutional Animal Care and Use Committee–approved protocol under anesthesia with isoflurane. Separate arms were treated with daily oral gavage of vehicle or ARN-509 (10 mg/kg/d) for 7 d.

PET imaging was conducted using an Inveon small-animal PET/CT scanner (Siemens) at 2 time points, once before treatment and once 7 d after treatment. The mice were injected with approximately 7.4 MBq of ^{68}Ga-PSMA via the tail vein. One hour after injection, they were anesthetized with 2% isoflurane and imaged for 10–20 min to acquire approximately 20 million coincident events. In the ARN-509–treated cohort, the PET acquisitions took place approximately 6 h after the final gavage within an energy window of 350–650 keV and a coincidence-timing window of 3.432 ns. The data were converted into 2-dimensional histograms, and images were reconstructed by filtered backprojection. After the PET acquisition, a coregistered CT scan was acquired within approximately 10 min. SUV_{mean} was calculated for each xenograft using manually segmented regions of interest, and the ratio of SUV_{mean} after treatment to SUV_{mean} before treatment was calculated for each animal.

Human Experiment

The local institutional review board approved the study, and written informed consent was obtained from the patient, a 51-y-old man who had castration-sensitive metastatic prostate cancer with a Gleason score of 10. He had received no treatment of any kind before the first PSMA PET study. For ADT, he received a single 7.5-mg intragluteal injection of leuprolide acetate (Lupron; AbbVie). He also received 50 mg of bicalutamide (Casodex; AstraZeneca) daily for 30 d.

The patient was imaged on a 3.0-T Signa PET/MRI scanner (GE Healthcare) at two time points, once before initiation of ADT and again 4 wk (29 d) after initiation. Imaging began an average of 97 minutes after injection of 207 ± 22 MBq (mean ± SD) of ^{68}Ga-PSMA-11. A 6-bed-position whole-body acquisition was performed from the mid thighs to the vertex for 3 min at each bed position. The PET data were reconstructed using time-of-flight information, ordered-subset expectation maximization with 2 iterations and 28 subsets, and a matrix size of 256 × 256. The PET transaxial and *z*-axis fields of view were 600 and 250 mm, resulting in a voxel size of 2.3 × 2.3 mm. Axial slices were reconstructed at a 2.78-mm thickness. Attenuation was corrected using a 2-echo Dixon fat–water separation algorithm for the body, whereas the lung was segmented using a region-growing algorithm provided with the scanner (*16*).

All lesions capable of segmentation at both time points were segmented using a semiautomated method. SUV_{max} was calculated for each lesion. If a lesion was seen on only the pretherapy images or only the posttherapy images, the volume of interest was placed in the same location on both sets of images and the SUV_{max} was recorded. SUV_{peak} and SUV_{mean} were not calculated, because many lesions were seen at only one time point, and therefore comparing SUV_{peak} and SUV_{mean} across two imaging studies was not feasible. All measurements were performed using an Advantage Workstation (version 5.0; GE Healthcare).

Statistical Analysis

A paired Student *t* test was used to compare SUV_{max} before and after ADT in the patient and in the mouse xenografts. An unpaired Student *t* test was used to compare the change in mouse xenograft SUV_{mean} between the treatment groups and the vehicle group.

RESULTS

Animal Experiment

No change in tumor SUV_{mean} was observed in the group treated with vehicle (Fig. 1: ratio, 0.90 ± 0.14; $P = 0.85$). Castration using orchiectomy resulted in an increase in SUV_{mean} (ratio, 1.55 ± 0.57; $P = 0.007$). Treatment with ARN-509 resulted in a larger increase in SUV_{mean} (ratio, 1.85 ± 0.44; $P = 0.013$).

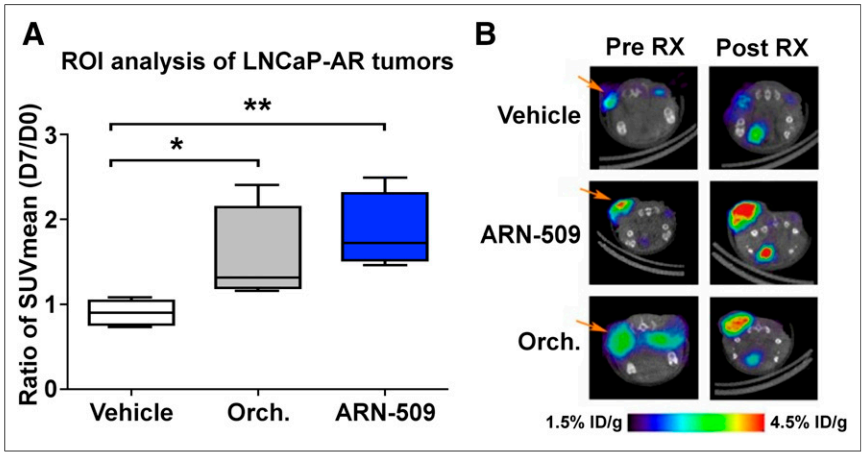

FIGURE 1. ^{68}Ga-PSMA-11 PET demonstrates increased PSMA expression in prostate cancer xenografts with inhibition of AR. (A) Ratio of SUV_{mean} at day 7 to day 0 increased an average of 72% with orchiectomy and 105% with ARN-509 compared with vehicle. (B) Visual assessment of ^{68}Ga-PSMA-11 PET demonstrates clear increase in uptake in xenografts in response to ARN-509 (middle row) and orchiectomy (bottom row), compared with controls treated with vehicle (top row). *$P = 0.007$. **$P = 0.013$. ID = injected dose; ROI = region of interest; RX = treatment.

Human Experiment

At 4 wk after the initiation of ADT, the patient's prostate-specific antigen level had decreased from 66.8 to 9.0 ng/mL. Imaging demonstrated a post-ADT increase in ^{68}Ga-PSMA-11 SUV_{max} from 2.9 ± 3.0 to 11.8 ± 6.9 (707% ± 689%) across 22 measurable lesions ($P < 0.001$) (Fig. 2). Of these 22 lesions, 13 that were thought to be visible on only the post-ADT PET images were found, in retrospect, to also be visible on the pre-ADT MR images (Fig. 3).

DISCUSSION

We have reconfirmed that AR inhibition can increase PSMA expression on PSMA PET in a mouse xenograft model, and for

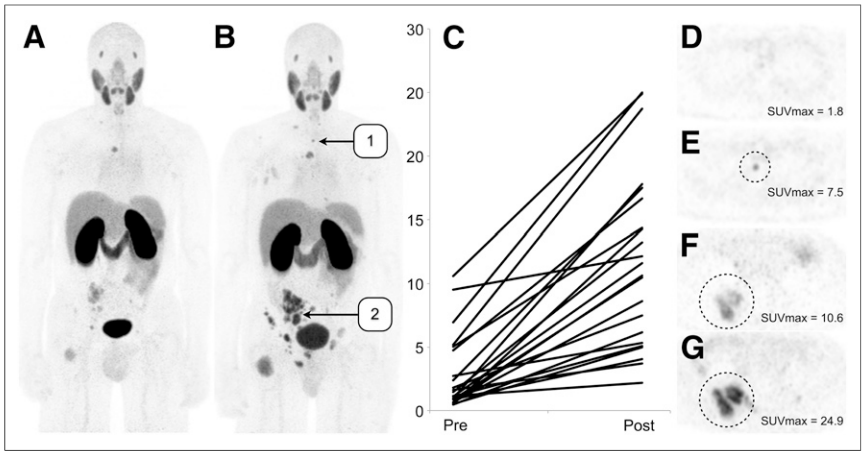

FIGURE 2. (A and B) Coronal maximum-intensity projections of patient with castration-sensitive metastatic prostate cancer imaged using ^{68}Ga-PSMA-11 before ADT (A) and after ADT (B) demonstrate marked increase in uptake in lesions. (C) Each visualized lesion demonstrated increased uptake, averaging more than 7 times the initial uptake. (D and E) Numerous lesions (13 of 22) were visualized only on posttreatment imaging, as exemplified by the upper thoracic osseous metastasis seen on these axial PET images. (F and G) Other lesions increased in size and had increased uptake on posttreatment imaging, as exemplified by the lesion seen on these axial PET images.

the first time, to our knowledge, we have shown that such an effect can also be demonstrated in humans.

Uptake in the patient was 7-fold higher at the post-ADT imaging time point than before treatment. This finding suggests that determining the post–AR inhibition imaging time point when PSMA expression is highest will be critical. Two processes are likely going on. The first is an increase in PSMA expression due to AR inhibition, as exhibited in our patient and as suggested recently by a study using ^{99m}Tc-MIP-1404 PSMA (*17*). The second is therapeutically induced cell death, which decreases the cell mass in the tumors and thus reduces their overall PSMA uptake. Previous work showed that a decrease in tumor mass can be seen on PSMA PET 4 mo after treatment with ADT (*18*). Although over 80% of patients respond to ADT, and chemical castration is typically achieved in 3–4 wk (*15,19–21*), the precise temporal relationship between initiation of ADT and PSMA expression remains unknown, as does the variation in this relationship between individual patients. Serial ^{68}Ga-PSMA-11 imaging of patients after AR inhibition is needed.

The temporal relationship between PSMA expression and initiation of ADT may explain the different detection sensitivities found for ^{68}Ga-PSMA-11 in patients with biochemical recurrence. Afshar-Oromieh et al. initially reported that detection sensitivity was increased in patients being treated with ADT (*8*), whereas Eiber et al. did not find a difference in detection sensitivity (*7*). A third study looked at a subpopulation of 4 patients who, like our patient, had castration-sensitive disease with falling prostate-specific antigen levels after treatment with ADT; all four demonstrated PSMA PET–positive disease (*5*).

These findings have several important implications. If PSMA expression in patients with prostate cancer can be upregulated by inhibiting the AR, then it should be possible to use PSMA PET to increase the sensitivity with which metastases are detected in biochemical recurrence patients. This possibility is supported by our finding that 13 additional lesions could be visualized on PSMA PET only after pretreatment with ADT. Additionally, one might be able to increase the uptake of PSMA in patients being treated with ^{177}Lu-PSMA (*22–24*). Groups have already demonstrated that the efficacy of PSMA-targeted therapies can increase when they are paired with AR-targeted therapies (*25*). One might also be able to use changes in PSMA expression to interrogate the efficacy of second- and third-generation AR-targeted therapies.

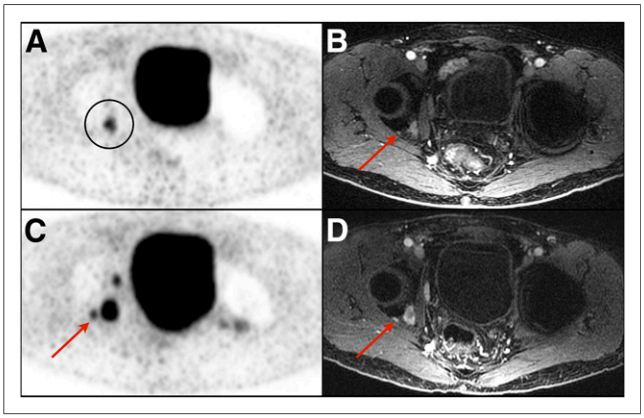

FIGURE 3. Examples of lesions seen only on post-ADT PSMA PET. (A) Pretreatment PET image demonstrates single lesion (circled) in right acetabulum. (B) Additional non–PSMA-avid right acetabular lesion (arrow) is seen just lateral to larger lesion on MR image of same location. (C) On post-ADT PET image, numerous additional lesions are seen, including adjacent acetabular lesion (arrow). (D) This lesion (arrow) is again demonstrated on enhanced T1-weighted MR image.

CONCLUSION

Inhibition of the AR can markedly change PSMA expression both in a mouse xenograft model and in clinical patients with castration-sensitive prostate cancer when imaged using ^{68}Ga-PSMA-11.

DISCLOSURE

Dr. Hope receives grant support, is on the speaker's bureau for GE Healthcare, and was supported by the Radiological Society of North America and the Department of Radiology and Biomedical Imaging, UCSF. Dr. Evans receives consulting fees, owns shares in ORIC Pharmaceuticals, Inc., and was supported by the 2013 David H. Koch Young Investigator Award from the Prostate Cancer Foundation, the National Institutes of Health (R00CA172695, 1R01CA17661), a Department of Defense Idea Development Award (PC140107), the UCSF Academic Senate, and GE Healthcare. Dr. Truillet was supported by a postdoctoral fellowship from the Department of Defense Prostate Cancer Research Program (PC151060). Research from UCSF reported in this publication was supported in part by the National Cancer Institute of the National Institutes of Health under award P30CA082103. No other potential conflict of interest relevant to this article was reported.

REFERENCES

1. Israeli RS, Powell CT, Corr JG, Fair WR, Heston WD. Expression of the prostate-specific membrane antigen. *Cancer Res.* 1994;54:1807–1811.
2. Silver DA, Pellicer I, Fair WR, Heston WD, Cordon-Cardo C. Prostate-specific membrane antigen expression in normal and malignant human tissues. *Clin Cancer Res.* 1997;3:81–85.
3. Osborne JR, Akhtar NH, Vallabhajosula S, Anand A, Deh K, Tagawa ST. Prostate-specific membrane antigen-based imaging. *Urol Oncol.* 2013;31:144–154.
4. Hijazi S, Meller B, Leitsmann C, et al. Pelvic lymph node dissection for nodal oligometastatic prostate cancer detected by ^{68}Ga-PSMA-positron emission tomography/computerized tomography. *Prostate.* 2015;75:1934–1940.
5. Ceci F, Uprimny C, Nilica B, et al. ^{68}Ga-PSMA PET/CT for restaging recurrent prostate cancer: which factors are associated with PET/CT detection rate? *Eur J Nucl Med Mol Imaging.* 2015;42:1284–1294.
6. Morigi JJ, Stricker PD, van Leeuwen PJ, et al. Prospective comparison of ^{18}F-fluoromethylcholine versus ^{68}Ga-PSMA PET/CT in prostate cancer patients who have rising PSA after curative treatment and are being considered for targeted therapy. *J Nucl Med.* 2015;56:1185–1190.
7. Eiber M, Maurer T, Souvatzoglou M, et al. Evaluation of hybrid ^{68}Ga-PSMA ligand PET/CT in 248 patients with biochemical recurrence after radical prostatectomy. *J Nucl Med.* 2015;56:668–674.
8. Afshar-Oromieh A, Avtzi E, Giesel FL, et al. The diagnostic value of PET/CT imaging with the ^{68}Ga-labelled PSMA ligand HBED-CC in the diagnosis of recurrent prostate cancer. *Eur J Nucl Med Mol Imaging.* 2015;42:197–209.
9. Afshar-Oromieh A, Malcher A, Eder M, et al. PET imaging with a [^{68}Ga] gallium-labelled PSMA ligand for the diagnosis of prostate cancer: biodistribution in humans and first evaluation of tumour lesions. *Eur J Nucl Med Mol Imaging.* 2013;40:486–495.
10. Evans MJ. Measuring oncogenic signaling pathways in cancer with PET: an emerging paradigm from studies in castration-resistant prostate cancer. *Cancer Discov.* 2012;2:985–994.
11. Evans MJ, Smith-Jones PM, Wongvipat J, et al. Noninvasive measurement of androgen receptor signaling with a positron-emitting radiopharmaceutical that targets prostate-specific membrane antigen. *Proc Natl Acad Sci USA.* 2011;108:9578–9582.
12. Wright GL, Grob BM, Haley C, et al. Upregulation of prostate-specific membrane antigen after androgen-deprivation therapy. *Urology.* 1996;48:326–334.
13. Meller B, Bremmer F, Sahlmann CO, et al. Alterations in androgen deprivation enhanced prostate-specific membrane antigen (PSMA) expression in prostate cancer cells as a target for diagnostics and therapy. *EJNMMI Res.* 2015;5:66.
14. Miyamoto DT, Lee RJ, Stott SL, et al. Androgen receptor signaling in circulating tumor cells as a marker of hormonally responsive prostate cancer. *Cancer Discov.* 2012;2:995–1003.
15. Hussain M, Tangen CM, Higano C, et al. Absolute prostate-specific antigen value after androgen deprivation is a strong independent predictor of survival in new metastatic prostate cancer: data from Southwest Oncology Group Trial 9346 (INT-0162). *J Clin Oncol.* 2006;24:3984–3990.
16. Wollenweber SD, Ambwani S. Comparison of 4-class and continuous fat/water methods for whole-body, MR-based PET attenuation correction. *IEEE Trans Nucl Sci.* 2013;60:3391–3398.
17. Vallabhajosula S, Jhanwar Y, Tagawa S, et al. ^{99m}Tc-MIP-1404 planar and SPECT scan: imaging biomarker of androgen receptor (AR) signaling and prostate specific membrane antigen (PSMA) expression [abstract]. *J Nucl Med.* 2016;57(suppl 2):1541.
18. Schlenkhoff CD, Gaertner F, Essler M, Hauser S, Ahmadzadehfar H. ^{68}Ga-labeled anti-prostate-specific membrane antigen peptide as marker for androgen deprivation therapy response in prostate cancer. *Clin Nucl Med.* 2016;41:423–425.
19. Seidenfeld J, Samson DJ, Hasselblad V, et al. Single-therapy androgen suppression in men with advanced prostate cancer: a systematic review and meta-analysis. *Ann Intern Med.* 2000;132:566–577.
20. Miyamoto H, Messing EM, Chang C. Androgen deprivation therapy for prostate cancer: current status and future prospects. *Prostate.* 2004;61:332–353.
21. Sharifi N, Gulley JL, Dahut WL. Androgen deprivation therapy for prostate cancer. *JAMA.* 2005;294:238–244.
22. Baum RP, Kulkarni HR, Schuchardt C, et al. ^{177}Lu-labeled prostate-specific membrane antigen radioligand therapy of metastatic castration-resistant prostate cancer: safety and efficacy. *J Nucl Med.* 2016;57:1006–1013.
23. Zechmann CM, Afshar-Oromieh A, Armor T, et al. Radiation dosimetry and first therapy results with a ^{124}I/^{131}I-labeled small molecule (MIP-1095) targeting PSMA for prostate cancer therapy. *Eur J Nucl Med Mol Imaging.* 2014;41:1280–1292.
24. Kratochwil C, Giesel FL, Stefanova M, et al. PSMA-targeted radionuclide therapy of metastatic castration-resistant prostate cancer with ^{177}Lu-labeled PSMA-617. *J Nucl Med.* 2016;57:1170–1176.
25. DiPippo VA, Nguyen HM, Brown LG, Olson WC, Vessella RL, Corey E. Addition of PSMA ADC to enzalutamide therapy significantly improves survival in in vivo model of castration resistant prostate cancer. *Prostate.* 2016;76:325–334.